HIGH-TEMPERATURE, PERHAPS SILICIC, VOLCANISM ON MARS EVIDENCED BY TRIDYMITE DETECTION IN HIGH-SIO₂ SEDIMENTARY ROCK AT GALE CRATER, MARS.

R.V. Morris[1], D.T. Vaniman[2], D.F. Blake[3], R. Gellert[4], S.J. Chipera[5], E.B. Rampe[6], D.W. Ming[1], S.M. Morrison[7], R.T. Downs[7], A.H. Treiman[8], A.S. Yen[9], C.N. Achilles[7], T.F. Bristow[3], J.A. Crisp[9], D.J. Des Marais[3], J.D. Farmer[10], K.V. Fendrich[7], J. Frydenvang[11], T.G. Graff[12], J.P. Grotzinger[13], J.M. Morookian[9], S.P. Schwenzer[14], and the MSL Science Team. [1]NASA JSC (richard.v.morris@nasa.gov), [2]PSI, [3]NASA ARC, [4]UofGuelph, [5]CHK Energy, [6]Aerodyne, [7]UofA, [8]LPI, [9]JPL/Caltech, [10]ASU, [11]LANL & UofCopenhagen, [12]Jacobs, [13]Caltech, [14]Open Univ.

Curiosity at Gale Crater: The Mars Science Laboratory (MSL) rover, Curiosity, has been exploring sedimentary rocks within Gale crater since landing in August, 2012. On the lower slopes of Aeolis Mons (a.k.a. Mount Sharp), drill powder was collected from a high-silica (74 wt% SiO_2) outcrop named Buckskin (BK). It was a surprise to find that the Buckskin sample contained significant amounts of the relatively rare silica polymorph tridymite. We describe the setting of the Buckskin sample, the detection of tridymite by the MSL Chemistry and Mineralogy (CheMin) X-ray diffraction instrument, and detection implications.

Geologic setting: The Buckskin outcrop is part of the Murray formation exposed in the Marias Pass area. The formation was previously studied by CheMin in the Pahrump Hills member [1] where three samples of drill fines were analyzed (Confidence Hills (CH), Mojave2 (MJ) and Telegraph Peak (TP) [2]). Assuming approximately horizontal bedding, the Buckskin outcrop is ~15 m stratigraphically above the bottom of the Pahrump Hills member. Mudstone, generally characterized by fine lamination, is the dominant depositional facies [1].

Buckskin Mineralogical and Chemical Composition: The CheMin instrument and XRD pattern analysis procedures have been previously discussed [3-6]. The diffraction pattern used for quantitative XRD analysis (Fig. 1) is the sum of the first 4 of 45 diffraction images. The remaining images are all characterized by both on-ring and off-ring diffraction spots that we attributed to poor grain motion and particle clumping. Coincident with particle clumping was a significant decrease in the intensity of the tridymite diffraction peaks (Fig. 2a). The derived mineralogical composition of the crystalline component (derived from the first 4 diffraction images) is given in Table 1. The tridymite is well-crystalline and its pattern is refined as monoclinic tridymite (Fig 1). Mineral chemical compositions were derived from XRD unit cell parameters or obtained from stoichiometry.

The XRD-calculated amorphous component was 50 ± 15 wt%. We constrained the value to 60 wt% because it is the minimum value necessary to give a positive Al_2O_3 concentration for the amorphous component using APXS data for the post-sieve dump pile (Table 2). The amorphous component has high SiO_2 (~77 wt%) and high anion ($SO_3+P_2O_5+Cl$ ~10 wt%) concentrations. Calculation shows that a cation-anion balance is achieved if the cations in the amorphous component

except SiO_2 and TiO_2, which do not readily form salts, are assumed to be present as amorphous mixed-cation sulfates, phosphates, and chlorides (or perchlorates/chlorates).

Table 1. Mineralogy of Buckskin drill fines (wt%).

	Crystalline Component	Bulk Sample[‡]	
		XRD	APXS
Plagioclase	42.8 ± 3.0	21.4 ± 1.5	17.1 ± 1.2
Sanidine	8.4 ± 1.8	4.2 ± 0.9	3.4 ± 0.7
Magnetite	6.9 ± 0.8	3.5 ± 0.4	2.8 ± 0.3
Anhydrite	1.8 ± 0.6	0.9 ± 0.3	0.7 ± 0.2
Tridymite	34.1 ± 2.0	17.1 ± 1.0	13.6 ± 0.8
Cristobalite	4.6 ± 0.8	3.0 ± 0.4	2.4 ± 0.3
Amorphous	---	50 ± 15[§]	60
Total	100	100	100

[‡]Amorphous component calculated from XRD patterns and from APXS chemistry.
[§]Includes contributions broad humps centered near 26º and 31º 2θ and low-angle scattering.

Fig. 1

Buckskin Frames 1-4

Refined as Monoclinic Tridymite [8]
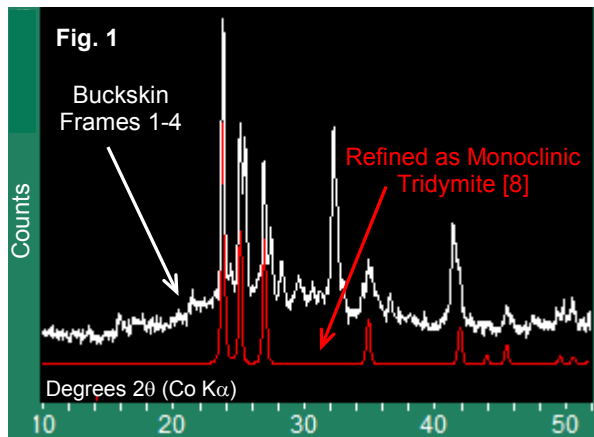
Counts

Degrees 2θ (Co Kα)

Fig. 2b shows individual diffraction patterns for CH, TP, BK, and Greenhorn (GH) which were calculated to the same integration time (sum of 45 images). The amorphous component is characterized by a broad hump centered near 26 °2θ, which implies a high-SiO_2 phase (e.g., any combination of silica to rhyolitic glass or opal-A) is present. This result is different from previous CheMin analyses where the amorphous hump is centered near 31 °2θ, consistent with any combination of basaltic glass and certain amorphous sulfates and phosphates [4-7]. Thus, the amorphous component of the Murray formation at CH, TP, and BK and the Stimson

formation at GH is dominated by a high-SiO_2 composition.

Tridymite, a high-temperature SiO_2 polymorph: Tridymite is the stable SiO_2 polymorph at low pressures and between 870 to 1700 °C [e.g., 9], can be prepared synthetically at those high temperatures using a variety of procedures [e.g., 10-12], and is metastable at low temperatures. In lunar and meteorite samples, subordinate tridymite is attributed to high temperature igneous and/or impact processes on parent bodies [e.g., 13-16]. Subordinate tridymite is also associated with some terrestrial impact structures [e.g., 17, 18].
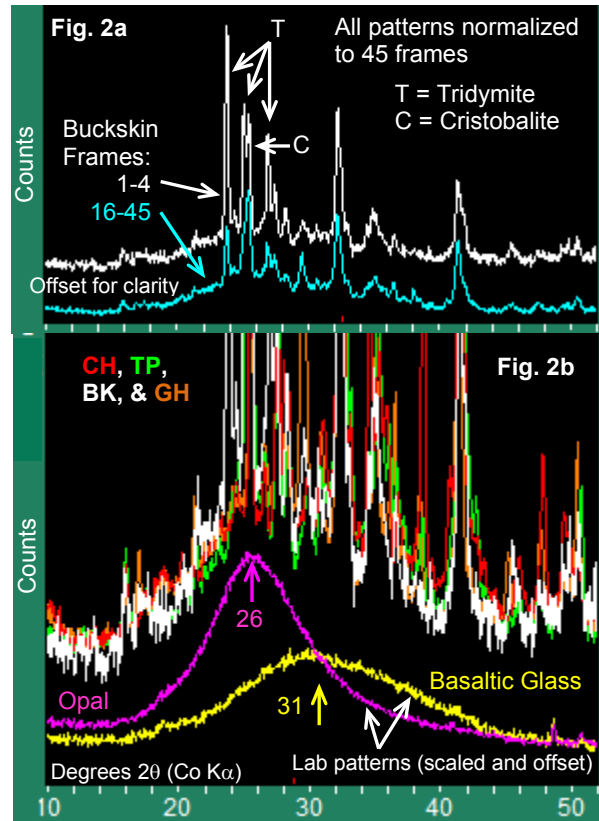
Table 2. Buckskin chemical compositions with 60 wt% amorphous component.

(wt%)	Crystalline	Bulk (APXS)	Amorphous
SiO_2	68.20	73.86	77.49
TiO_2	0.12	1.61	2.59
Al_2O_3	13.91	5.54	0.03
Cr_2O_3	0.00	0.09	0.15
FeOT	7.25	5.40	4.29
MnO	0.00	0.06	0.11
MgO	0.16	0.77	1.17
CaO	5.25	3.01	1.53
Na_2O	2.80	2.04	1.54
K_2O	1.35	0.97	0.72
P_2O_5	0.00	1.27	2.10
SO_3	1.06	4.81	7.28
Cl	0.00	0.28	0.47
Total	100.10	99.77	99.47

Significant tridymite concentrations are associated with terrestrial basaltic through rhyolitic volcanism. At basaltic Stromboli volcano, the high-SiO_2 residue of acid sulfate leaching is the progenitor of pyrometamorphic ejecta that has up to 90 wt% tridymite [19]. High-SiO_2 progenitors by way of acid-sulfate leaching are reported in other volcanic settings [e.g., 20, 21]. At andesitic Soufriere Hills volcano, high concentrations of tridymite + cristobalite were found in fine grained (<125 µm) pyroclastic flows and associated ash plumes generated by lava dome collapse [22]. An ash-flow unit associated with the rhyolitic Bandelier Tuff has 25 wt% tridymite [23]. In a lacustrine setting whose catchment includes basaltic-andesite to rhyolitic volcanics, clastic sediments with ~70 wt% SiO_2 have cristobalite + tridymite concentrations upwards from 30% [24].

Silicic volcanism on Mars: In the absence of a geologically credible low-temperature formation process, BK tridymite (~14 wt% relative to bulk sample) implies high temperatures and a high-SiO_2 progenitor. Progenitors include residues of acid-sulfate leaching and silicic volcanism. The tridymite and amorphous component might be process coupled as discussed above for terrestrial volcanism. We consider it unlikely that high-SiO_2 material plus tridymite was delivered to the Murray formation as impact ejecta. In any case, BK tridymite

(and also TP cristobalite) is interpreted as detrital. The high-SiO_2 amorphous component (silicic glass or opal-A) could be either detrital if process-coupled with tridymite or diagenetic if independently formed (e.g., a chemical precipitate [25] or an opaline residue of acid sulfate leaching). A clast akin to BK (tridymite + silicic glass + SO_3) with possible martian origin is present in a polymict ureilite meteorite and interpreted as evidence for silicic volcanism [26].

Fig. 2a — All patterns normalized to 45 frames. T = Tridymite, C = Cristobalite. Buckskin Frames: 1-4, 16-45. Offset for clarity.

Fig. 2b — CH, TP, BK, & GH. Opal. Basaltic Glass. Lab patterns (scaled and offset). Degrees 2θ (Co Kα).

References: [1] Grotzinger et al. (2015) *Science 350*, 6257. [2] Rampe et al., This Meeting. [3] Blake et al. (2012) *SpSciRev*, DOI 10.1007/s11214-11012-19905-11211. [4] Bish et al. (2013) *Science 283*, 1142. [5] Vaniman et al. (2013) *Science*, DOI:10.1126/ science.1243480. [6] Treiman et al. (2016) submitted. [7] Morris et al. (2015) *LPSC46* #2434. [8] Graetsch and Topalovic-Dierdorf (1996) *EJMin 8*, 103 [9] Swamy et al. (1994) *JGR-SE 99*, 11787. [10] Sato (1963) *MineralJ 4*, 115. [11] Shinohara and Kohyama (2004) *IndHealth 42*, 277. [12] Chen et al. (2005) *ISIJ Inter 45*, 791. [13] Bridges et al. (2005) *Meteoritics 30*, 715. [14] Treiman et al. (2004) *EPSL, 219*, 189. [15] Seddio et al. (2015) *AmMin 100*, 1533. [16] Xirouchakis et al. (2002) *GCA 66*, 1867. [17] Whitehead et al. (2002) *M&PS 37*, 623. [18] Jackson et al. (2011) *AmMin 96*, 81. [19] Del Moro et al. (2011) *JPetrol 52*, 541. [20] Getahun et al. (1996) *JVolGeothermRes 71*, 73. [21] Frolova et al. (2010) *ProcWorldGeoCongress, 1.* [22] Baxter et al. (1999) *Science 283,* 1142. [23] Broxton et al. (1995) LANL Rept. LA-12934-MS. [24] Roy et al. (2009) *GeochemJ 43*, 49. [25] Ramseyer et al. (2013) *M&P Geo 39*, 187. [26] Beard et al. (2015) *M&PS 50,* 1613.